

## Development and evaluation of virtual instrument to supplement ultrasonic echoscope system for ophthalmology

R. Jurkonis<sup>1</sup>, V. Marozas<sup>1,2</sup>, S. Kurapkienė<sup>3</sup>

<sup>1</sup>*Institute of Biomedical Engineering, Kaunas University of Technology*

<sup>2</sup>*Signal processing department, Kaunas University of Technology*

<sup>3</sup>*Dept. of Ophthalmology of Institute for Biomedical Research of Kaunas University of Medicine*

### Abstract

The aim of this paper was twofold: first, to present a virtual instrument for characterization of the cataract severity in the lens of the eye, based on the indirect measurements of ultrasound attenuation coefficient, second, to evaluate the instrument *in vitro* by assessment of measurement errors in case of the four different phantoms with a priori known characteristics (pure water, castor oil, soybean oil, plexiglass) and measurement conditions (distance to the lens or sample in phantoms). We demonstrated that such virtual instrument can be built by using standard PC, ultrasonic transducer for ophthalmology, the shelf digitizer (Picoscope ADC 212/100, Picotech Ltd.), laboratory generator and popular software package LabView (National Instruments Inc.). The instrument is able to process acquired data and assess the attenuation coefficient of the material or tissue in real time and would be able to provide the ophthalmologist with the timely feedback. Results of the *in vitro* experiments show that the random error (precision of measurements) of the attenuation coefficient estimates is proportional to the absolute value of the coefficients and can possibly limit the power of the method to characterize the lens state at advanced cataract stages. While the systematic error (accuracy of measurements), which is due to ultrasound beam diffraction, limits the possibilities to use the method for early detection of cataract. More sophisticated ultrasound signal processing methods must be developed in order to reduce attenuation coefficient estimation uncertainty.

**Keywords:** cataract, ultrasound attenuation coefficient, virtual instrument.

### Introduction

The eye lens cataract is a very frequent ocular pathology, which is difficult to diagnose at early stages and to describe quantitatively by means of slit-lamp microscopy. Ultrasonic tissues characterization approach showed promising possibilities to quantitatively and non-invasively estimate the degree of cataract [1, 2, 3]. Authors of study [4] demonstrated the value of ultrasound attenuation coefficient as the descriptor of diabetic cataract severity. The age related changes in the lens of human eye were investigated using ultrasound attenuation measurement approach [5]. The results suggest the possibility to detect cataract in its early stages.

A lot of the research is done in tissue characterization using ultrasound transmission technique [6] and pulse-echo technique: [7, 8, 9, 10, 11]. In these papers, research is aimed to estimate attenuation parameters in: a-priori known materials, *in-vitro* eye tissues, *in-vivo* liver tissue, to obtain parametric B-mode images indicating mean attenuation coefficient in heterogeneous tissue, to develop experimental diffraction corrections using interface multiple reflections pulses, but specific paper on eye tissue characterization it has not been yet published to our knowledge.

Proprietary ultrasonic echoscope systems have many features for common ophthalmological investigations in a routine clinical practice. However, ophthalmology researchers, physicians and surgeons at university hospitals are looking for advanced investigation and diagnosis methods that are not yet available in commercial systems. The advanced diagnosis methods can be developed and deployed on additional hardware and software supplementing the proprietary echoscope. In study [3], we used a benchtop digital storage oscilloscope together with proprietary *Mentor*<sup>TM</sup> A/B ultrasonic imaging system

(Advent, Norwell, MA) for acquisition of echograms and MATLAB software package for off-line signal processing. The time consuming signal acquisition, storage, and manual processing of the ultrasound signals have motivated us to develop a new system for characterization of lens cataract.

Virtual instrumentation concept introduced by National Instruments Inc. already 20 years ago is gaining popularity. Virtual instrument is a program that implements functions of an instrument by a computer and a signal digitizer. The well known software package LabView is mostly used to develop a software of virtual instruments.

The present paper describes the development and evaluation of the new virtual instrument dedicated to eye lens tissue characterization using attenuation frequency function. The modified instrument is based on the high speed (100MHz), high resolution (12 bits) digitizer Picoscope ADC 212/100 (Picotech Ltd) and a custom built software in LabView. The developed software is able to process the acquired data in the real time and present the estimated ultrasound attenuation coefficient for further diagnostic decisions. The second aim of the study was to estimate the ultrasound beam diffraction contribution into overall error of the attenuation coefficient measurement. This paper clarifies diffraction distortion issue and would cancel doubt and debate.

The proposed virtual instrument development and evaluation methodology can be transferred to other medical applications to decelerate the depreciation of the expensive medical equipment.

### Materials and methods

The general idea of the virtual instrument supplementing the proprietary system is presented in Fig 1.

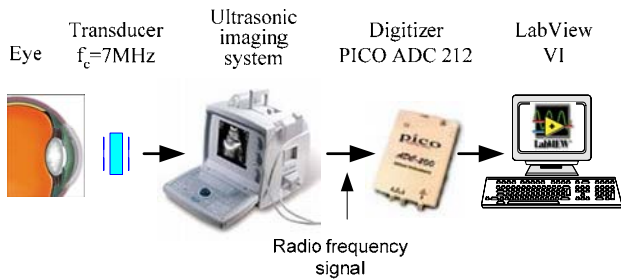


Fig.1. The structure of a virtual instrument supplementing the ultrasonic ophthalmology system for characterization of eye lens cataract

The echography signals are sent and received by the proprietary 7 MHz A-scan ultrasonic imaging system *Mentor*<sup>TM</sup> A/B (Advent, Norwell, MA). The analog radio frequency signals are acquired to PC using the PC oscilloscope PICO ADC-212/100 (Pico Technology Ltd., Cambridgeshire, UK) with the 100 MHz sampling frequency and 12 bits amplitude resolution. All signal processing and analysis is implemented in a software using the LabVIEW virtual instrument methodology and it is described later in the paper.

The goal of instrument evaluation was to investigate the feasibility of estimation of ultrasound attenuation coefficient in different materials and to test the impact of ultrasound beam diffraction to results of the measurements.

The experimental setup for evaluation of the instrument is shown in Fig. 2. The generator G5-15 was used to trigger the ultrasound pulse generator (HM8131-2) and the digitizer of received pulses. The transducer was excited by modulated pulses: duration- 0,1  $\mu$ s, frequency - 7 MHz, amplitude- 20 V. Such excitation pulses ensures echo pulses similar to pulses which are obtained in a live eye echography [3]. The LabView based program controls all the equipment.

The impact of ultrasound beam diffraction was investigated by changing the distance between the transducer and phantom. The displacement was ensured with a manual micro-screw, equipped with a micrometer. The 0,05 mm displacement step was used in all experiments.

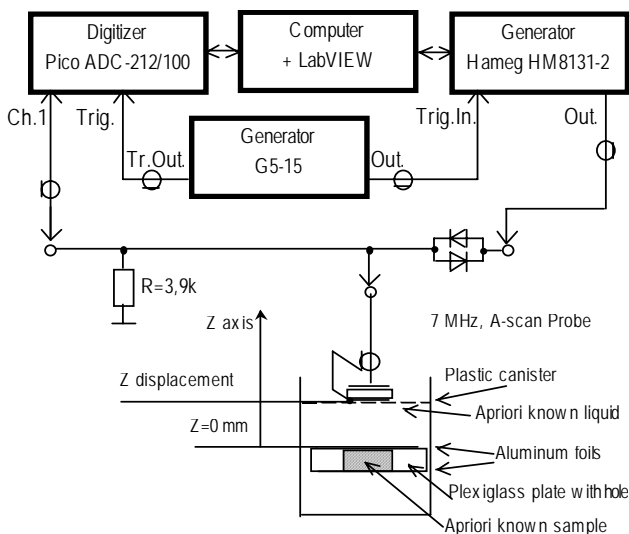


Fig.2. Experimental setup for evaluation of the virtual instrument

The evaluation procedure consisted of series of *in vitro* experiments. There were four phantoms used. Plain layers of material (samples) surrounded with fluid were imitating the lens of the eye. The fluid allowed shift of the transducer along the acoustic axis, so that the distance between the transducer and the sample under investigation could be changed. Change of the distance enabled us to asses the impact of the ultrasound beam diffraction to the measurements of attenuation coefficient. The simplest phantom (No.2) was a plexiglas plate immersed in the container with water. Other three samples were made of plexiglas plates with 15mm diameter holes filled with liquid materials (see Table 1). The bottoms of the holes were completely covered with foils, but only partially covered at the top in order to allow the air bubbles to leave the sample liquid. The hole covering foils surrounded by fluid ensure strong reflected pulses from the sample anterior and posterior surfaces. The foils do not distort spectra of the reflected ultrasonic pulse because of their small thickness (about 10  $\mu$ m).

Table 1. Summary of parameters of phantom materials and human eye lens tissue

| Phantom material, or eye tissue                                     | Distance $z_d$ , or thickness of sample $z_s$    | Attenuation frequency function $\alpha = \beta f^y$ , dB / MHz <sup>y</sup> cm | Frequency range and reference | Extrapolated attenuation coefficient $\beta_{7MHz}$ , dB / MHz <sup>1,0</sup> cm |
|---|--|--|-------------------------------|--|
| Filling liquid  |  |  |                               |  |
| Water, used in phantom No.1, 2 and 4                                | $z_d = 1 \dots 14$ mm                            | 0.0024 dB/cm/MHz <sup>2,0</sup> ; $y=2,0$                                      | $f=1,0 \dots 45,0$ MHz; [12]  | 0,03 dB / cm / MHz   |
| Soybean oil, used in phantom No.3                                   |  | no reference data  |                               |  |
| Separating films  |  |  |                               |  |
| Aluminum foil, used in phantom No.1, 3 and 4                        | $z_{s,af} = 10$ $\mu$ m                          | not considered   |                               |  |
| Sample material   |  |  |                               |  |
| Water, used in phantom No.1.  | $z_{s,w} = z_{s,p} = z_{s,so} = z_{s,co} = 4$ mm | see above  |                               |  |
| Plexiglas (or PMMA - polymethylmethacrylate), used in phantom No.2. |  | 0,94 dB/cm/MHz <sup>1,00</sup> ; $y=1,0$                                       | $f=0,5 \dots 5,0$ MHz; [13]   | 0,94 dB / cm / MHz   |
| Soybean oil, used in phantom No.3.                                  |  | no reference data  |                               |  |
| Castor oil, used in phantom No.4.                                   |  | 0,7 dB/cm/MHz <sup>1,67</sup> ; $y=1,67$                                       | $f=0,5 \dots 5,0$ MHz; [13]   | 4,30 dB / cm / MHz   |
|   | 0,81 dB/cm/MHz <sup>1,67</sup> ; $y=1,67$        | $f=0,5 \dots 3,5$ MHz; [14]  | 4,85 dB / cm / MHz            |  |
|   | 0,69 dB / cm MHz <sup>1,66</sup> ; $y=1,66$      | $f=9 \dots 19$ MHz; [15]   | 4,07 dB / cm / MHz            |  |
| Eye tissues   |  |  |                               |  |
| Lens, no visual signs of cataract                                   |  | 0,1 dB / cm MHz <sup>2</sup> ; $y=1,87$  | $f=17 \dots 23$ MHz; [7]      | 1,03 dB / cm / MHz   |

The first (phantom No.1) and the third (phantom No.3) samples were filled with water and soybean oil and left for one day in order degas. The fourth sample (No.4) hole was carefully filled with castor oil ensuring no visible bubbles. Then the hole was completely covered with foil. Because castor oil is viscous enough, the foil remained plastered even when frame was immersed into a canister with water.

The attenuation coefficients of the materials used in experiments were found in the literature. However, the frequency bands that were used for measurements in the references are different than that used in our ultrasonic eye A-scan probe (the central frequency 7 MHz, the frequency band from  $f_1=6$  MHz to  $f_2=8$  MHz). Thus, the comparison of the measured and literature based data would not be feasible. We solved this issue by using linear extrapolation of the published attenuation coefficients to our frequency band.

The complete description of all phantom related parameters is summarized in Table 1.

### Ultrasonic signal processing method

The ultrasonic signal processing scheme is explained in Fig. 3.

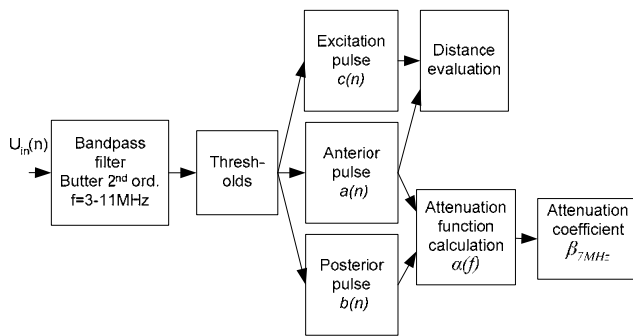


Fig.3. Ultrasonic signal processing for estimation of attenuation coefficient

First, in order to reduce the noise, the acquired echogram was digitally filtered using Butterworth bandpass 2-nd order filter with  $f_{low}=3$  MHz and high  $f_{high}=11$  MHz cut-off frequencies. Then, the echogram passed through the amplitude threshold detector, which selected parts of the waveform belonging to echo pulses from anterior and posterior foils. The values of thresholds were found empirically, e.g. in the case of the castor oil sample (phantom No.4), the thresholds were: 10mV, 2 mV and 1 mV for excitation, anterior and posterior pulses, respectively. The waveforms of anterior and posterior pulses were used for calculation of the attenuation function in the frequency domain. In order to increase the frequency resolution, both waveforms were zero padded up to 4096 samples. The selected waveforms of pulses consists of 20 samples before threshold instant and 128 samples in long. To improve detector immunity to a noise the a-priori time ranges in the echogram were set. So, the beginning of echogram (1,4  $\mu$ s) and delay in the sample layer (4 $\mu$ s) were excluded from analysis in peak detectors. Both waveforms after FFT are represented as amplitude (not power) spectra. The amplitude spectra were individually normalized to have a maximum magnitude of 1. Then the logarithm of the attenuation function is calculated. The

signal processing procedure until now is summarized in the following expression:

$$\alpha(f) = 20 \log \frac{|FFT[a_1(t)]| / \text{MAX}\{FFT[a_1(t)]\}}{|FFT[a_2(t)]| / \text{MAX}\{FFT[a_2(t)]\}} \quad (1)$$

Here  $a_1(t)$  is the echo pulse from the anterior foil,  $a_2(t)$  is the echo pulse from posterior foil,  $FFT$  is the fast Fourier transform.

The attenuation coefficient of the sample under investigation is associated to the slope of the estimated attenuation function:

$$\beta_{7MHz} = LSF[\alpha(f)] / (2Z_s(f_2 - f_1)) \quad (2)$$

Here:  $LSF[*]$  – mean least square fit;  $Z_s$  - thickness of the sample layer, i.e.  $Z_s=4$  mm;  $(f_2 - f_1)$  – selected frequency range, in our case  $(f_2 - f_1)=2$  MHz. This finalizes calculation of the attenuation coefficient.

The dependence of the attenuation coefficient as the function of displacement between the ultrasonic transducer and the sample under investigation was evaluated. In order to increase the precision of  $\beta$  estimates, 100 of measurement trials were accomplished at each transducer displacement point. A mean and standard deviation of the coefficients were calculated and stored.

During data collection the displacements were evaluated automatically using parallel signal processing branch according to this equation:

$$d = \frac{vt_{ea}}{2} \quad (3)$$

Here  $t_{ea}$  - the delay time between excitation and anterior pulses detected,  $v$ - the speed of ultrasound in the transmission fluid. As in the case of the attenuation coefficient estimation, 100 of measurements were collected for estimation of the mean and standard deviation at each transducer displacement point.

### Results

An example of echographic data processing steps is shown in Fig.4. The example presents the case when the lens phantom with the castor oil sample and water as transmission liquid were investigated. The transducer was displaced from the sample by  $Z_d=14$  mm in this case, therefore the echogram signal to noise ratio was the worst in all cases investigated (Fig.4a). The band pass filtering helped to remove the excessive noise from the echogram (Fig. 4b). The large central frequency shift can be observed in the amplitude spectra of the posterior pulse in comparison with the anterior pulse (Fig. 4c). We can see that the monotonic attenuation function has local extreme points, which we suppose are originating from non-ideal homogeneity of the sample material and non-ideal planar reflector made from aluminum foil.

The main results of virtual instrument evaluation are presented in Fig. 5. There are shown experimental distributions of the attenuation coefficient along the acoustic beam in four a priori known phantoms. Bold lines illustrate the mean value, while the error bars – the standard deviation of the measured attenuation coefficients. This diagram clearly illustrates contribution of the diffraction into inaccuracy of the attenuation coefficient estimation.

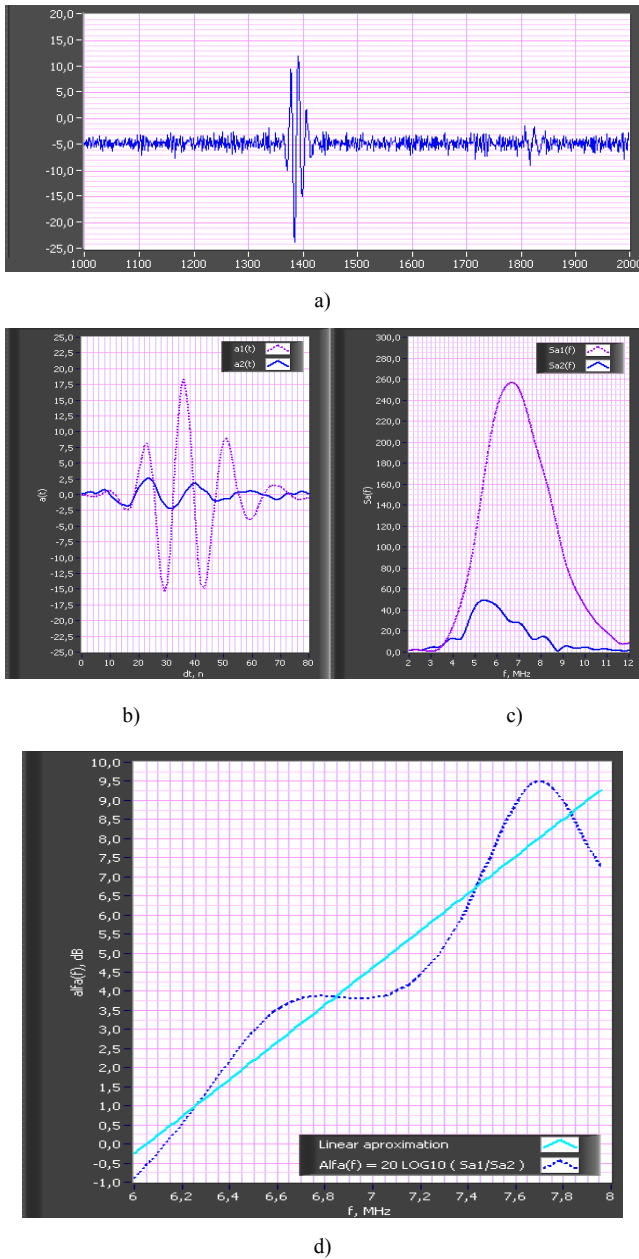


Fig.4. Diagrams illustrating processing of echography signal from phantom No.4: a - raw waveform of received echogram; b - filtered and selected pulses of anterior and posterior aluminum foils and c - their amplitude spectra; d - calculated attenuation function.

Statistics summarizing the experiments is presented in Table 2. The parameters of the echo pulses used in the attenuation coefficient estimation algorithm were also evaluated for random errors. The evaluated parameters were: 1) peak-to-peak voltage of anterior ( $U_{ppa}$ ) and posterior ( $U_{ppp}$ ) pulses from the sample; 2) sample thickness ( $z_s$ ) estimated from the delay time between the anterior and posterior echo pulses; 3) the distance between the transducer and the sample ( $z_d$ ) estimated from delay time between the excitation pulse and the anterior echo pulse. The means of the experimental attenuation coefficients are presented as global averages (first averaging in time, then along the distance). The standard

deviation values are estimated after time averaging. The experimental attenuation coefficients agree well with the reference data in Table 2.

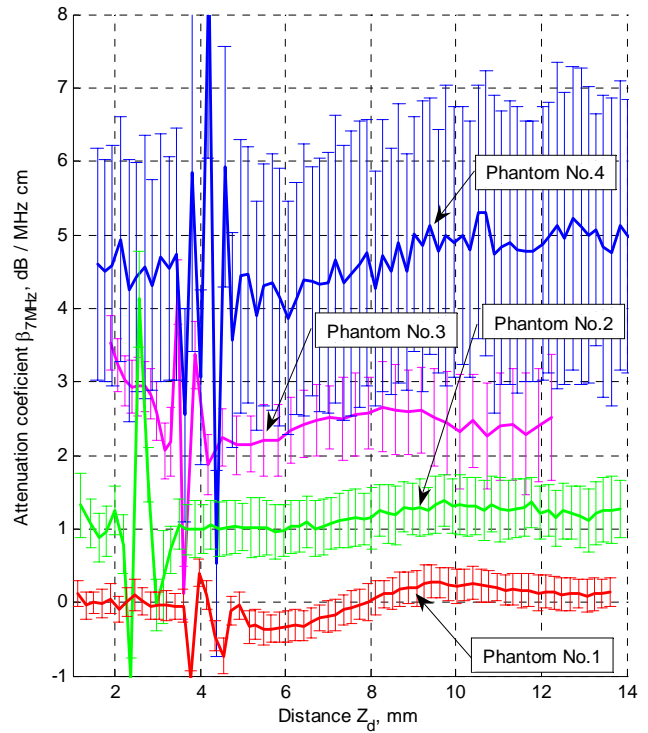


Fig.5. Estimated attenuation coefficients as the function of the distance between transducer face and phantom sample. Here: phantom No1- pure water, phantom No2- plexiglas, phantom No3- soybean oil, phantom No4- castor oil

Table 2. Summary of parameters registered from phantoms and comparison of the estimated attenuation coefficient with the reference data

| Phantom number | Percent deviations about the means |               |           |           | The means and std values of the attenuation coefficient estimates |                          | Reference data of attenuation coefficients |
|----------------|------------------------------------|---------------|-----------|-----------|---|--------------------------|--|
|                | $U_{ppas}$ , %                     | $U_{ppp}$ , % | $z_s$ , % | $z_d$ , % | $\langle \beta \rangle$ , dB/cm MHz                               | $std(\beta)$ , dB/cm MHz |  |
| 1              | 1,25                               | 1,22          | 2,11      | 0,45      | 0,01  | 0,26                     | 0,03 [12]                                  |
| 2              | 1,32                               | 2,72          | 0,21      | 0,25      | 1,13  | 0,48                     | 0,94 [13]                                  |
| 3              | -                                  | -             | 0,11      | 0,15      | 2,59  | 0,65                     | -  |
| 4              | 1,78                               | 10,1          | 1,65      | 0,26      | 4,75  | 0,82                     | 4,07...4,85 [13,14,15]                     |

Comparing the obtained attenuation coefficient with the reference data we can state, that attenuation coefficient estimation accuracy is acceptable for Plexiglas and castor oil. The standard deviation values in the range 0,2...10% show that primary parameters of echo pulses, such as: pulse peak-peak voltage, sample thickness, displacement between the transducer and the sample are estimated with a relatively small random error. However, the attenuation coefficient or secondary parameter of echo pulses are estimated with a relatively big random error of level 35...45%.

## Discussion

The feasibility to supplement the proprietary ultrasound system with additional advanced functions is investigated. Specifically, we proposed to utilize the analog front-end of the old ultrasound imaging system in order to build the new instrument with the advanced function, namely, the estimation of ultrasound attenuation coefficient for characterization of the lens tissue in human eye. Little additional hardware is needed in this solution. The advanced function itself can be implemented in a software using LabView virtual instrument paradigm.

A number of studies [1, 2, 3, 7, 9] have used *in vivo* experiments for investigation of ultrasound attenuation in tissues of the eye. In our case, the evaluation of the developed instrument was accomplished using *in vitro* experiments. The usage of known artificial phantoms enabled us to limit the number of error sources, which otherwise could be countless when *in vivo* experiments. Still, several sources of errors limit the accuracy and precision of attenuation coefficient estimation even in the case of controlled *in vitro* experiments.

The increasing random error of the estimated attenuation coefficient can be observed when the absolute value of the coefficient increases (see Fig. 5). This result can be interpreted as being caused by decreasing the signal to noise ratio when the attenuation of the material increases. Nevertheless, the random error can be minimized by using averaging of multiple measurements.

Large, repeating in all phantoms, disturbances of the attenuation coefficient can be seen in the range of distances from 2 to 5 mm (Fig. 5). These disturbances are caused by multiple reflections and interferences among the reflected pulses. We think that the large differences of acoustic impedances in phantom materials are responsible for above-mentioned effects. These conditions are hardly possible to occur in live tissues, which have small impedance differences.

The systematic component of the error is seen in the results of attenuation coefficient estimation as the function of the displacement between the transducer and the sample in the phantom (Fig.5). We admit and agree with [16] that this error is being caused by ultrasound beam diffraction effects. It can be observed the repeating pattern of this error in all phantoms. This observation suggests the possibility to compensate for this kind of error. We leave this issue for another research.

The power of the ultrasound test to diagnose the lens cataract at its early stage depends on the uncertainty of the ultrasound attenuation coefficient estimation and the knowledge of the normality limits of the attenuation coefficient measure for normal lenses. Sugata [2] found the normal human lens attenuation to be 0.07-0.92 dB/cmMHz, while in different cataract types 1.6-7.3 dB/cmMHz, and expressed the idea about quantitative and early detection of cataract from echo signals. Our results confirm this hypothesis. However, the observed increase of the uncertainty in larger attenuation coefficients estimates limits the possibilities for quantitative characterization of the lens state in advanced cataract. More sophisticated ultrasonic signal processing approaches must be sought in order to decrease the inherent uncertainty.

Researchers publish that the human eye lens tissue attenuation coefficient is age dependent. Korte [7] have obtained linear regression analysis results, which show that in the frequency range  $f = 17...23$  MHz the attenuation coefficient slope at 20 MHz is  $\beta_{20\text{MHz}} = 0,64 + 0,0093/\text{year}$  [dB/cmMHz]. This finding contributes to our presumption about that value in normal human eye lens not less than 0,5 [dB/cmMHz], where diffraction distortion does not contribute the bigger systematic error than the unavoidable random error.

The lens tissue attenuation parameters from several researchers [1, 2, 3, 7, 9] are hardly comparable because of different frequency ranges investigated. In addition, the results of these investigations are affected by different apertures of the transducers used. Thus, we would encourage further research on attenuation estimation in weakly attenuating materials using the presented method.

## Conclusions

1. A software based tool, a virtual instrument, supplementing functionality of a commercial echography system for ophthalmology is developed and evaluated.
2. The eye tissue characterizing tool is evaluated *in vitro* on the phantoms with well documented acoustic attenuation coefficients of a-priori known materials such as: water, polymethylmethacrylate (Plexiglas), and castor oil.
3. The evaluated A-scan probe with the diameter of 5mm and the moderate (7 MHz) ultrasonic center frequency show the diffraction distortion contribution into the error of attenuation coefficient estimations is not bigger than the random error contribution within the range of the distance  $Z = 1 \dots 12$  mm from the transducer till sample layer, if the estimated coefficient is not less than 1 dB/cmMHz.
4. Taking into account the hard conditions in life eye echoscopy and therefore a large random error, the evaluated systematic inaccuracy of cataract lens tissue characterizing system is acceptable for a clinical use.

## References

1. Oguchi Y., Van Marle G.W., Eijkskoot F. and Henkes H.E. Study of the ultrasonic characteristics of the lens. *Bibl. Ophthalmol.* 1975. Vol.83. P.37-40.
2. Sugata Y., Murakaami K., Masayasu I. and Yamamoto Y. An application of ultrasonic tissue characterization to the diagnosis of cataract. *Acta Ophthalmol.* 1992. Vol.70. Suppl.204. P. 35-39.
3. Paunksnis A., Kuzmienė L., Kurapkienė S., Jurkonis R., Ivanov L., Sadauskienė I., Lukoševičius A. and Jegelevičius D. Ultrasonic and biochemical characteristics of human nuclear cataract. *Ultrasound.* 2001. Vol.3(40). P.11-15.
4. Paunksnis A., Kurapkienė S., Mačiulis A., Raitelaitienė R., Jurkonis R. and Lukoševičius A. Estimation of ultrasound attenuation coefficient of human diabetic cataract. *Ultrasound.* 2003. Vol.1(46). P.37-40.
5. Raitelaitienė R., Kurapkienė S., Mačiulis A. and Paunksnis A. The influence of age related changes to ultrasound attenuation of human eye lens. *Ultrasound.* 2004. Vol.2(51). P.55-59.
6. He P. Experimental verification of models for determining dispersion from attenuation. *IEEE Trans. Ultrason. Ferroelec. Freq. Contr.* 1999. Vol. 46. No.3. P.706-714.

7. **Korte C. L., De Steen A. F. W. van der and Thijssen J. M.** Acoustic velocity and attenuation of eye tissues at 20 MHz. *Ultrasound in Med. & Biol.* 1994. Vol.20. No.5. P.471-480.
8. **Kuc R.** Bounds on estimating the acoustic attenuations of small tissue regions from reflected ultrasound. *Proc. of the IEEE.* 1985. Vol. 73. No.7. P.1159-1169.
9. **Ye S. G., Harasiewicz K. A., Pavlin C. J. and Foster F. S.,** Ultrasound characterization of normal ocular tissue in the frequency range from 50 MHz to 100 MHz. *IEEE Trans. Ultrason. Ferroelec. Freq. Contr.* 1995. Vol.42. No.1. P.8-14.
10. **Jirik R., Taxt T. and Jan J.,** Ultrasound attenuation imaging. *J. Elec.Eng.* 2004. Vol.55. No.7-8. P.180-187.
11. **Lerch T. P., Cepel R. and Neal S. P.** Attenuation coefficient estimation using experimental diffraction corrections with multiple interface reflections. *Ultrasonics.* 2006. Vol.44.P.83-92.
12. **Filipczynski L., Kujawska T., Tymkiewicz R. and Wojcik J.** Nonlinear and linear propagation of diagnostic ultrasound pulses. *Ultrasound in Med. & Biol.* 1999. Vol.25. No.2. P.285-299.
13. **Hep.** Experimental verification of models for determining dispersion from attenuation. *IEEE Trans. Ultrason. Ferroelec. Freq. Contr.* 1999. Vol.46. No.3. P.706-714.
14. **Liebler M., Ginter S., Dreyer T. and Riedlinger R. E.** Full wave modeling of therapeutic ultrasound: Efficient time-domain implementation of the frequency power-law attenuation. *J. Acoust. Soc. Am.* 2004. Vol.116 (5). P.2742-2750.
15. **Jurkonis R.** Investigation of time transformations of signals in ultrasonic medical diagnostics. Doctor dissertation., KTU. 2000. P.101. (in Lithuanian).
16. **Cespedes I. and Ophir J.** Correction of diffraction errors in attenuation estimation with dynamic beam translation. *Ultrasound in Med. & Biol.* 1992. Vol.18. No.2. P.213-218.

R. Jurkonis, V. Marozas, S. Kurapkienė

#### **Oftalmologinę echoskopinę sistemą papildančio virtualaus prietaiso kūrimas ir tyrimas**

Reziumė

Darbo tikslas - sukurti virtualų prietaisą kataraktos pažeistiems lęšiuko audiniams tirti ultragarsu, registruojant ultragarso silpimo

koeficientą ir in-vitro apibrėžti tokiu prietaisu registruojamų įverčių tikslumą, esant žinomų medžiagų fantomams ir žinomoms echoskopavimo sąlygoms.

Metodai. Parodyta galimybė sudaryti virtualų prietaisą asmeninio kompiuterio bazėje, naudojant oftalmologinį ultragarsinį keitiklį, signalų skaitmenizatorių Picoscope ADC 212/100, Picotech Ltd., laboratorinį generatorių ir populiarų programų paketą LabView National Instruments Inc.

Virtualus prietaisas realiuoju laiku apdoroja ultragarsinį signalą ir apskaičiuoja silpimo medžiagoje arba biologiniame audinyje koeficientą. Ultragarso silpimo koeficiento įverčių tikslumas nustatytas keturiais akies lęšiuko fantomais, pagamintais iš vandens, organinio stiklo, sojos ir ricinų aliejaus.

Rezultatai. *In vitro* tyrimo rezultatai rodo, kad atsitiktinė silpimo koeficiento įverčio paklaida yra proporcinga užregistruotai absoliučiajai koeficiento vertei ir gali apriboti metodo tinkamumą lęšiuko audiniams, esant pribrendusiai kataraktai, apibūdinti. Tuo tarpu sisteminė paklaida, kurią lemia ultragarso difrakcija, apriboja metodo taikymą ankstyvajai kataraktos stadijai diagnozuoti. Todėl, taikant ultragarso silpimo koeficiento įvertinimą, lęšiuko audiniams charakterizuoti, reikia toliau tirti signalų apdorojimo metodus.

Išvados. Virtualaus instrumento pagrindu sukurta ir išbandyta programinė įranga, papildanti komercinių ultragarsinių oftalmologinių sistemų funkcionalumą. Akies audinį charakterizuojanti įranga yra išbandyta *in vitro* su fantomais, kai naudojamos medžiagos (vanduo, organinis stiklas, ricinų aliejus), kurių ultragarso silpimo koeficientas yra gerai žinomas ir dokumentuotas.

A-skenavimo 5 mm skersmens keitiklio, esant 7 MHz centriniam ultragarsiniam dažniui, tyrimas  $z = 1 \dots 12$  mm atstumų tarp keitiklio ir pavyzdinės medžiagos diapazone rodo, kad difrakcinių iškraipymų sistemingasis indėlis į silpimo koeficiento įverčio paklaidą yra ne didesnis už atsitiktinę paklaidą, jeigu koeficiento įverčio vertė ne mažesnė už 1 dB/cm MHz.

Atsižvelgiant į tai, kad gyvos akies echoskopavimo sąlygos yra sudėtingos ir todėl gaunamos didelės atsitiktinės paklaidos, ištirtasis lęšiuko audinio charakterizavimo metodo sisteminis tikslumas yra priimtinas klinikiniam taikymui.

Pateikta spaudai 2007 03 05